Available online at www.sciencedirect.com
ScienceDirect
Journal of Computational Physics 227 (2008) 2293–2316
JOURNAL OF COMPUTATIONAL PHYSICS
www.elsevier.com/locate/jcp

Stable and accurate schemes for the compressible Navier–Stokes equations

K. Mattsson [a,b,*], M. Svärd [a,c], M. Shoeybi [a]

[a] Center for Turbulence Research, Building 500, Stanford University, Stanford, CA 94305-3035, United States
[b] Department of Information Technology, Uppsala University, Uppsala, SE 751 05 Uppsala, Sweden
[c] Centre of Mathematics for Applications, University of Oslo, P.B 1053, Blindern N-0316 Oslo, Norway

Received 24 July 2006; received in revised form 5 October 2007; accepted 15 October 2007
Available online 1 November 2007

Abstract

Minimal stencil width discretizations of combined mixed and non-mixed second-order derivatives are analyzed with respect to accuracy and stability. We show that these discretizations lead to stability for Cauchy problems. With a careful boundary treatment, we also show that the stability holds for initial-boundary value problems. The analysis is verified by numerical simulations of Burgers' and Navier–Stokes equations in two and three space dimensions.

Keywords: Compressible; Minimal stencil width schemes; Navier–Stokes equations; Numerical stability; Boundary conditions; Second-derivatives

1. Introduction

Minimal stencil width approximations of non-mixed second-derivatives have long been known to have good accuracy properties. However, stability cannot easily be proven for problems with a combination of mixed ($\partial^2/\partial x\partial y$) and non-mixed ($\partial^2/\partial x^2$, $\partial^2/\partial y^2$) second-derivatives, such as the compressible Navier–Stokes equations and the elastic wave equation [7]. In this paper, we introduce the term *narrow*, to define explicit finite difference schemes with a minimal stencil width.

For the continuous problem one can derive an energy estimate for the linearized and symmetrized Navier–Stokes equations, proving boundedness of the initial-boundary value problem [18,16,4]. (Although the analysis in this paper is done for a 2-D problem, the extension to a 3-D problem is straightforward.) If first-derivative difference operators that satisfy a summation-by-parts (SBP) formula are employed twice for all second-derivatives (non-mixed and mixed, yielding a wide stencil approximation), and if the simultaneous approximation term (SAT) method [3] is used to implement the boundary conditions, one can

* Corresponding author. Address: Center for Turbulence Research, Building 500, Stanford University, Stanford, CA 94305-3035, United States. Tel.: +1 650 723 0546; fax: +1 650 723 9617.
E-mail address: mattsson@stanford.edu (K. Mattsson).

0021-9991/$ - see front matter
doi:10.1016/j.jcp.2007.10.018

exactly mimic the continuous energy estimate (proving stability, see [4]). However, the wide-stencil approximation does not damp spurious oscillations (the highest frequency that can exist on the grid) without addition of artificial dissipation.

Stability is not so easily shown for a narrow-stencil approximation of the Navier–Stokes equations. However, if stability can be shown, the advantage of using a narrow-stencil approximation compared to the corresponding wide-stencil approximation is twofold: (i) The narrow-stencil approximation have a smaller error coefficient and (ii) it damps the highest frequency mode (spurious oscillations), without the addition of artificial dissipation. Hence, the narrow-stencil approximation is potentially more accurate than a wide-stencil approximation, in particular when viscous effects are important.

The main focus in this paper is to prove stability for narrow-stencil approximations of the compressible Navier–Stokes equations. A detailed discussion on efficiency (see [10,14] for a more precise definition of efficiency) in terms of runtime for a given error tolerance is avoided here, since is it relies to much on the actual problem and code implementation. The results for the 2-D Burgers' equation (that is also analyzed and simulated in this paper) show that the narrow-stencil approximations are much more accurate than the wide-stencil approximations on a given grid. The fact that the stencil width is naturally smaller, means that less arithmetic operations are needed on a given grid using a narrow-stencil. The time-step restrictions using an explicit Runge–Kutta method are almost identical for both formulations. Hence, the narrow-stencil approximations of the 2-D Burgers' equation are more efficient than the wide-stencil approximations. The second-order accurate simulations of the compressible Navier–Stokes equations also indicate that the narrow-stencil approximation is more efficient than the wide-stencil approximation. A more extensive analysis is required before any decisive conclusions can be made for the high-order accurate narrow-stencil approximations of the compressible Navier–Stokes equations. (Such a code has not yet been implemented.)

Stable and high-order accurate narrow SBP approximations for 1-D problems were analyzed in [13]. However, stability for 2-D and 3-D problems with mixed second-derivative terms were never addressed in [13].

In Section 2, we discuss the SBP property for the first- and second-derivative difference operators. In Section 3 we show an important relationship between the first- and second-derivative SBP operators, referred to as *compatibility*. The first main result in this paper is to prove that a certain group of the SBP operators presented in [13] can become compatible. The second main result is to prove that compatibility is a necessary condition obtaining an energy estimate (i.e., proving stability) for the narrow-stencil approximation of the Navier–Stokes equations. A 2-D model of the Navier–Stokes equations is introduced where we show how to combine the SAT method and the SBP operators to obtain stable narrow-stencil approximations using the energy method [5]. In Section 4, the accuracy of the narrow- and wide-stencil approximations are compared by performing numerical simulations of Burgers' and the compressible Navier–Stokes equations in 2-D and 3-D. Conclusions are drawn in Section 5.

2. Definitions

The 2-D and 3-D schemes are constructed using 1-D SBP finite difference operators. We begin with a short description and some definitions (for more details, see [8,19,13]).

Let the inner product for real-valued functions $u,v \in L^2[0,1]$ be defined by $(u,v) = \int_0^1 uvw\,dx$, $w(x) > 0$, and let the corresponding norm be $\|u\|_w^2 = (u,u)$. The domain $(0 \leqslant x \leqslant 1)$ is discretized using $N+1$ equidistant grid points,

$$x_i = ih, \quad i = 0, 1 \ldots, N, \; h = \frac{1}{N}.$$

The approximative solution at grid point x_i is denoted v_i, and the discrete solution vector is $v^{\mathrm{T}} = [v_0, v_1, \ldots, v_N]$. Similarly, we define an inner product for discrete real-valued vector functions u, $v \in \mathbf{R}^{\mathbf{N+1}}$ by $(u,v)_H = u^{\mathrm{T}} H\, v$, where $H = H^{\mathrm{T}} > 0$, with the corresponding norm $\|v\|_H^2 = v^{\mathrm{T}} H v$. The following vectors will be frequently used:

$$e_0 = [1, 0, \ldots, 0]^{\mathrm{T}}, \quad e_N = [0, \ldots, 0, 1]^{\mathrm{T}}. \tag{1}$$

2.1. Narrow-diagonal SBP operators

To define narrow-diagonal SBP operators, we make use of the following definition:

Definition 2.1. An explicit pth-order accurate finite difference scheme with minimal stencil width of a Cauchy problem, is called a pth-order accurate narrow stencil.

Remark. We say that a scheme is explicit if no linear system of equations need to be solved to compute the difference approximation. Spatial Padé discretizations [11] are often referred to as "compact schemes". The approximation of the derivative is obtained by solving a tri- or penta-diagonal system of linear equations at every time-step. Hence, if written on explicit form, Padé discretizations lead to full difference stencils, similar to spectral discretizations.

Consider the hyperbolic scalar equation $u_t + u_x = 0$ (excluding the boundary condition). Multiplying by u and integrating by parts (referred to as the energy method) lead to

$$\frac{\mathrm{d}}{\mathrm{d}t}\|u\|^2 = -(u,u_x) - (u_x,u) = -u^2|_0^1, \tag{2}$$

where $u^2|_0^1 \equiv u^2(x=1) - u^2(x=0)$.

Definition 2.2. A difference operator $D_1 = H^{-1}Q$ approximating $\partial/\partial x$, using a pth-order accurate narrow-stencil, is said to be a pth-order accurate narrow-diagonal first-derivative SBP operator, if H is diagonal and positive definite, and $Q + Q^{\mathrm{T}} = B = \mathrm{diag}(-1,0,\ldots,0,1)$.

As an example of its use, consider the semi-discretization of $u_t + u_x = 0$, which is $v_t + D_1 v = 0$. Multiplying by $v^{\mathrm{T}}H$ from the left and adding the transpose lead to

$$\frac{\mathrm{d}}{\mathrm{d}t}\|v\|_H^2 = -(v,H^{-1}Qv)_H - (H^{-1}Qv,v)_H = -v^{\mathrm{T}}(Q+Q^{\mathrm{T}})v = v_0^2 - v_N^2. \tag{3}$$

Estimate (3) is the discrete analog of (2).

For parabolic problems, we need an SBP operator for the second derivative. Consider the heat equation

$$u_t = (bu_x)_x, \tag{4}$$

where $b(x) > 0$ is a smooth function. Multiplying (4) by u and integrating by parts lead to

$$\frac{\mathrm{d}}{\mathrm{d}t}\|u\|^2 = (u,(bu_x)_x) + ((bu_x)_x,u) = 2buu_x|_0^1 - 2\|u_x\|_b^2. \tag{5}$$

Definition 2.3. Let $D_2^{(b)} = H^{-1}(-M + BS)$ approximate $\partial/\partial x(b\partial/\partial x)$, where $b(x) > 0$ is a smooth function, using a pth-order accurate narrow-stencil. $D_2^{(b)}$ is said to be a pth-order accurate narrow-diagonal second-derivative SBP operator, if H is diagonal and positive definite, M is symmetric and positive semi-definite, S approximates the first-derivative operator at the boundaries and $B = \mathrm{diag}(-b_0,0,\ldots,0,b_N)$.

(High-order accurate narrow-diagonal second-derivative SBP operators for constant coefficients $b(x) = 1$, denoted D_2, were constructed in [13].) An example of its use is the semi-discretization $v_t = D_2^{(b)}v$ of (4). Multiplying by $v^{\mathrm{T}}H$ and adding the transpose lead to

$$\frac{\mathrm{d}}{\mathrm{d}t}\|v\|_H^2 = 2v_N(BSv)_N + 2v_0(BSv)_0 - 2v^{\mathrm{T}}Mv. \tag{6}$$

Estimate (6) is a discrete analog of (5).

Remark. To obtain energy estimates for schemes utilizing both D_1 and $D_2^{(b)}$ requires that both are based on the same norm H.

There are two options in obtaining a narrow-stencil approximation of (4). The first option (as shown above) is to approximate $(b\,u_x)_x$ using a narrow-diagonal second-derivative SBP operator $D_2^{(b)}$, to exactly mimic the continuous estimate (5). This yields a strictly stable approximation (see [5] for the exact definition of strict stability), meaning that the continuous and discrete energy-growth (or decay) are consistent. (A second-order accurate narrow-diagonal second-derivative SBP operator $D_2^{(b)}$ is presented in Appendix C). The second approach is to discretize the expanded form $bu_{xx} + b_x u_x$ (using the constant coefficient SBP operators in [13]), given by $v_t = \overline{B}D_2 v + \overline{B}_x D_1 v$. The matrices $\overline{B}$, $\overline{B}_x$ have the values of b, b_x injected on the diagonal. Multiplying $v_t = \overline{B}D_2 v + \overline{B}_x D_1 v$ by $v^{\mathrm{T}}H$ and adding the transpose lead to

$$\frac{\mathrm{d}}{\mathrm{d}t}\|v\|_H^2 = 2v_N(BSv)_N + 2v_0(BSv)_0 + v^{\mathrm{T}}(Q^{\mathrm{T}}\overline{B}_x + \overline{B}_x Q - \overline{B}M - M^{\mathrm{T}}\overline{B})v. \tag{7}$$

Estimate (11) mimics the continuous estimate (5), if $(Q^{\mathrm{T}}\overline{B}_x + \overline{B}_x Q - \overline{B}M - M^{\mathrm{T}}\overline{B})$ is negative semi-definite. An eigenvalue analysis (not shown here) for various test-functions $b(x) > 0$ (and number of unknowns) indicate that $(Q^{\mathrm{T}}\overline{B}_x + \overline{B}_x Q - \overline{B}M - M^{\mathrm{T}}\overline{B})$ is negative semi-definite for the higher order approximations (but for the eighth-order accurate scheme we found cases with a small positive eigenvalue approaching zero when grid-refining).

However, a strictly stable approximation of the 1-D problem (4) does not automatically lead to a strictly stable approximation of

$$u_t = (c_{11}u_x + c_{12}u_y)_x + (c_{21}u_x + c_{22}u_y)_y,$$

modeling the viscous Navier–Stokes terms in 2-D. We will return to the stability issues for narrow-stencil approximations of 2-D and 3-D problems in Section 3.

Remark. The boundary closure for a pth-order accurate narrow-diagonal SBP operator is of order $p/2$ (see [13]). This means that the boundary closure for $(D_1)^2$ is of order $p/2 - 1$. Hence, for fully parabolic problems the global order of accuracy (for the wide-stencil approximation) drops to $(p/2 + 1)$th-order. The convergence rate for narrow-stencil approximations of incompletely parabolic problems like the Navier–Stokes equations (see [22] for more information on the accuracy of finite difference approximations) drops to $(p/2)$th-order. This means that narrow-stencil approximations of fully and incompletely parabolic problems have a global order of accuracy one order higher than corresponding wide-stencil approximations, except for the second-order accurate case where both formulations lead to second-order convergence.

2.2. 2-D domains

Next, we turn to 2-D schemes where the Kronecker product is needed

$$C \otimes D = \begin{bmatrix} c_{0,0}D & \cdots & c_{0,q-1}D \\ \vdots & & \vdots \\ c_{p-1,0}D & \cdots & c_{p-1,q-1}D \end{bmatrix},$$

where C is a $p \times q$ matrix and D is an $m \times n$ matrix. Two rules for the Kronecker product are used, $(A \otimes B)(C \otimes D) = (AC) \otimes (BD)$ and $(A \otimes B)^{\mathrm{T}} = A^{\mathrm{T}} \otimes B^{\mathrm{T}}$.

Next, consider the domain Ω defined as $0 \leqslant x \leqslant 1$, $0 \leqslant y \leqslant 1$ with an $(N+1) \times (M+1)$-point equidistant grid as

$$x_i = ih_x, \quad i = 0, 1 \ldots, N, \quad h_x = \frac{1}{N},$$

$$y_j = jh_y, \quad j = 0, 1 \ldots, M, \quad h_y = \frac{1}{M}.$$

The numerical approximation at grid point (x_i, y_j) is denoted $v_{i,j}$. We define a discrete solution vector $v^{\mathrm{T}} = [v^0, v^1, \ldots, v^N]$, where $v^k = [v_{k,0}, v_{k,1}, \ldots, v_{k,M}]$ is the solution vector at x_k along the y direction, illustrated in Fig. 1. To simplify the notation we introduce $v_{w,e,s,n}$ to define the boundary values at the west, east, south

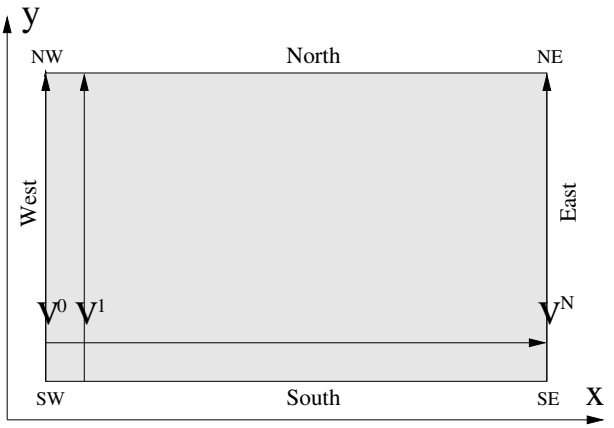

Fig. 1. Domain 2-D.

and north boundaries (see Fig. 1). In order to distinguish whether a difference operator P is working in the x or the y direction we will use the notations P_x and P_y. The following 2-D operators will frequently be used:

$$\begin{aligned} &D_x = (D_1 \otimes I_y), \quad D_y = (I_x \otimes D_1), \\ &D_{2x}^{(b)} = (D_2^{(b)} \otimes I_y), \quad D_{2y}^{(b)} = (I_x \otimes D_2^{(b)}), \\ &H_x = (H \otimes I_y), \quad H_y = (I_x \otimes H), \end{aligned} \tag{8}$$

where D_1, $D_2^{(b)}$ and H are the 1-D operators. $I_{x,y}$ are the identity matrices of appropriate sizes in the x and y direction, respectively. We also introduce the 2-D norm $\overline{H} \equiv H_x H_y$.

3. Analysis

We will introduce the main idea of this article with a 1-D model problem, before we go on with more interesting 2-D equations.

3.1. Compatible SBP operators

Consider the heat equation $u_t = u_{xx}$. The energy method leads to

$$\frac{\mathrm{d}}{\mathrm{d}t}\|u\|^2 = 2uu_x|_0^1 - 2\|u_x\|^2. \tag{9}$$

By discretizing $u_t = u_{xx}$ with a narrow-diagonal first-derivative SBP operator D_1 twice, we obtain the semi-discrete approximation $v_t = H^{-1}(-D_1^{\mathrm{T}} H D_1 + B D_1)v$. The energy method leads to

$$\frac{\mathrm{d}}{\mathrm{d}t}\|v\|_H^2 = 2v_N(D_1 v)_N - 2v_0(D_1 v)_0 - 2(D_1 v)^{\mathrm{T}} H (D_1 v). \tag{10}$$

Formula (10) exactly mimics (9), except for the highest frequency mode (see [15]). If we instead use the narrow-diagonal second-derivative SBP operator D_2, we obtain the semi-discrete approximation $v_t = H^{-1}(-M + BS)v$ of $u_t = u_{xx}$, leading to

$$\frac{\mathrm{d}}{\mathrm{d}t}\|v\|_H^2 = 2v_N(Sv)_N - 2v_0(Sv)_0 - 2v^{\mathrm{T}} M v. \tag{11}$$

Estimate (11) is a somewhat more vague approximation of (9), since the term $-v^{\mathrm{T}} M v$ is only known to be non-positive (see [13]). However, the advantage with narrow-diagonal second-derivative SBP operators is that they damp the highest frequency mode. We would like to relate M to $D_1^{\mathrm{T}} H D_1$, to understand the nature of the estimate (11). This is the key (as we will show later in this section) in order to derive stable narrow-stencil

approximations of the compressible Navier–Stokes equations in 2-D and 3-D. The goal for the rest of this section is to show that $M = D_1^{\mathrm{T}} H D_1 + R$, and prove that R is positive semi-definite.

The following definition is central in this paper:

Definition 3.1. Let D_1 and D_2 be pth-order accurate narrow-diagonal first- and second-derivative SBP operators. If $D_2 = H^{-1}(-D_1^{\mathrm{T}} H D_1 - R^{(p)} + BS)$, and the remainder $R^{(p)}$ is positive semi-definite, D_1 and D_2 are called *compatible*.

Lemma 3.2. *For the Cauchy problem, the remainder $R^{(p)}$ (see Definition 3.1) up to eighth-order accuracy is positive semi-definite.*

Proof. One can derive the following relations for the remainders $R^{(p)}$ ($p = 2,4,6,8$):

$$\begin{aligned}
-R^{(2)} &= -\frac{h^3}{4} D_4, \\
-R^{(4)} &= +\frac{h^5}{18} D_6 - \frac{h^7}{144} D_8, \\
-R^{(6)} &= -\frac{h^7}{80} D_8 + \frac{h^9}{600} D_{10} - \frac{h^{11}}{3600} D_{12}, \\
-R^{(8)} &= +\frac{h^9}{350} D_{10} - \frac{h^{11}}{2520} D_{12} + \frac{h^{13}}{14700} D_{14} - \frac{h^{15}}{78400} D_{16},
\end{aligned} \tag{12}$$

where $D_{2n} = (D_+ D_-)^n$ is an approximation of $\frac{\mathrm{d}^{2n}}{\mathrm{d}x^{2n}}$. For example, $(D_+ D_- v)_j = (v_{j+1} - 2v_j + v_{j-1})/h^2$ is the second-order accurate narrow second-derivative finite difference approximation. By using Fourier analysis, it is easily shown (see, for example, [15]) that $-R^{(p)}$ constitutes only dissipative terms. □

Hence, we have shown that the wide-stencil plus a dissipative term is equal to the narrow-stencil for a Cauchy problem. This was expected since the narrow-stencil damps the highest frequency mode.

For initial-boundary value problems we need to close the schemes at the boundaries with one-sided stencils. For the second-order accurate case (see Appendix C) we have

$$R^{(2)} = \frac{1}{h} \begin{bmatrix}
\frac{1}{4} & -\frac{1}{2} & \frac{1}{4} & & & & & \\
-\frac{1}{2} & \frac{5}{4} & -1 & \frac{1}{4} & & & & \\
\frac{1}{4} & -1 & \frac{3}{2} & -1 & \frac{1}{4} & & & \\
 & \frac{1}{4} & -1 & \frac{3}{2} & -1 & \frac{1}{4} & & \\
 & & & \ddots & & & & \\
 & & \frac{1}{4} & -1 & \frac{3}{2} & -1 & \frac{1}{4} & \\
 & & & \frac{1}{4} & -1 & \frac{5}{4} & -\frac{1}{2} & \\
 & & & & \frac{1}{4} & -\frac{1}{2} & \frac{1}{4} &
\end{bmatrix}. \tag{13}$$

The following Theorem can be proven (see Appendix A):

Theorem 3.3. *Let A be an $n \times n$ penta-diagonal symmetric matrix. Assume $\sum_{j=1}^{n} A_{ij} = 0$ and $A_{ii} > 0$, $A_{i,i+1} < 0$, $A_{i,i+2} > 0$. If $-A_{1,2} \geqslant 2A_{1,3}$, $-A_{n,n-1} \geqslant 2A_{n,n-2}$ and $-A_{i,i+1} \geqslant 2A_{i-1,i+1} + 2A_{i,i+2}$, $i = 2 \ldots n-2$, then A is positive semi-definite.*

Corollary 3.4. *The matrix, $R^{(2)}$, given by (13) is positive semi-definite.*

Proof. The conditions in Theorem 3.3 can easily be verified. □

SBP operators often include free parameters that can be tuned. For the second- and fourth-order accurate narrow-diagonal SBP operators, there are no free parameters. For the sixth- and eighth-order accurate narrow-diagonal SBP operators, the number of free parameters in D_1 are one and three, respectively.

The sixth-order accurate D_1 operator (see Appendix C) has one free parameter x_1. The original choice for x_1 (see [19]) was done to raise the truncation error to fourth-order at one boundary point (of totally 6). That choice however does not lead to a positive definite $R^{(6)}$, which can be found by a numerical eigenvalue analysis. There are other properties to consider (besides compatibility), such as spectral radius (see, for example, [21]) and accuracy. To find an good value for the free parameter x_1 we perform a numerical search, "optimizing" (we do not claim that we have a global optimum) for accuracy, spectral radius and compatibility, leading to $x_1 = \simeq 0.70127127127$. (We identify that there is a strong correlation between accuracy, spectral radius and compatibility, see Fig. 2.) A numerical study reveals that there is an interval

$$x_1 \in [0.6789094547\ 0.7254477238], \tag{14}$$

where $R^{(6)}$ is positive semi-definite, see Fig. 2.

In the eighth-order accurate case, D_1 has three free parameters (see Appendix C). The following values:

$$x_1 = 0.6978947368, \quad x_2 = -0.1205263157, \quad x_3 = 0.7586842105,$$

lead to $R^{(8)} \geqslant 0$. An eigenvalue analysis is not a strict proof, since it does not necessarily hold for an arbitrary number of grid points. However, in the fourth- and sixth-order cases it is possible pose a stronger statement. (In the eighth-order case we have not been able to work out a stronger proof than the eigenvalue analysis.)

Proposition 3.5. *$R^4 \geqslant 0$ and, $R^6 \geqslant 0$ with $x_1 = 0.70127127127$ for any number of grid points.*

Proof. See Appendix B. □

The first main result of this paper is stated in the following Theorem:

Theorem 3.6. *With proper choices of the free parameters in D_1, the second-, fourth- and sixth-order accurate narrow-diagonal SBP operators are compatible.*

Proof. See Corollary 3.5 and Proposition 3.4. □

3.2. Stability of a linearized Burgers' equation in 2-D

The main focus in this paper is to show that compatibility is a necessary condition obtaining an energy estimate (i.e., stability) for the compressible Navier–Stokes equations, which in 2-D can be written as

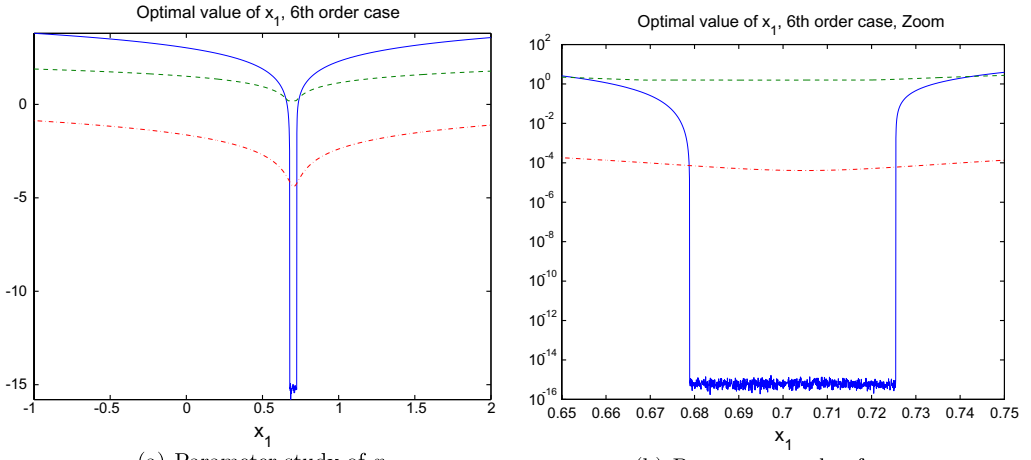

(a) Parameter study of x_1 (b) Parameter study of x_1,zoom

Fig. 2. A numerical study of varying x_1. Solid line (log-scale) is the largest positive eigenvalue of $-R$; the dashed line is the spectral radius of D_1 and the dashed-dotted shows the error (in l_2) of D_1 applied to a test function.

$$\tilde{u}_t + F_x + G_y = (\widetilde{C}_{11}\tilde{u}_x + \widetilde{C}_{12}\tilde{u}_y)_x + (\widetilde{C}_{21}\tilde{u}_x + \widetilde{C}_{22}\tilde{u}_y)_y, \quad [x,y] \in \Omega,\ t \geqslant 0. \tag{15}$$

To introduce the basic ideas, we begin the analysis by considering the 2-D Burgers' equation

$$u_t + \left(\frac{u^2}{2}\right)_x + \left(\frac{u^2}{2}\right)_y = (c_{11}u_x + c_{12}u_y)_x + (c_{21}u_x + c_{22}u_y)_y, \quad [x,y] \in \Omega,\ t \geqslant 0, \tag{16}$$

which is a model of (15). We expand the second-derivative terms to obtain

$$u_t + \left(\frac{u^2}{2}\right)_x + \left(\frac{u^2}{2}\right)_y = c_{11}u_{xx} + (c_{12}u_y)_x + (c_{21}u_x)_y + c_{22}u_{yy} + (c_{11})_x u_x + (c_{22})_y u_y, \quad [x,y] \in \Omega,\ t \geqslant 0. \tag{17}$$

We linearize around the exact solution $\bar{u}$ by introducing $u = \bar{u} + u'$,

$$u'_t + \bar{u}u'_x + \bar{u}u'_y = c_{11}(\bar{u})u'_{xx} + (c_{12}(\bar{u})u'_y)_x + (c_{21}(\bar{u})u'_x)_y + c_{22}(\bar{u})u'_{yy} + (c_{11}(\bar{u}))_x u'_x + (c_{22}(\bar{u}))_y u'_y. \tag{18}$$

By freezing the coefficients in (18), we obtain

$$u'_t + au'_x + bu'_y = c_{11}u'_{xx} + c_{12}u'_{yx} + c_{21}u'_{xy} + c_{22}u'_{yy}, \quad [x,y] \in \Omega,\ t \geqslant 0, \tag{19}$$

where $a = \bar{u}$, $b = \bar{u}$ and c_{ij} are now frozen coefficients. Note that $(c_{11}(\bar{u}))_x = (c_{22}(\bar{u}))_y = 0$ since $\bar{u} = constant$. The linearization of the non-split form (16) and the expanded form (17) is naturally the same (when freezing the coefficients). Well-posedness for both of those formulations follows if (19) is well-posed for all a, b in the range of $\bar{u}$ and similarly for the second-derivative terms. (For more information on this linearization procedure see [9,5,1].)

Remark. We will prove that the perturbation u' stays bounded. By freezing the coefficients in (18) we have discarded lower-order terms. Those lower order terms will contribute to a potential growth of the perturbation u', but the additional growth of the lower order terms will always be bounded (see for example [17]). Moreover, the growth due to the linearization for any problem with a small viscosity ($c_{ij} \ll \bar{u}$) will mainly come from the convective terms with the strongest non-linearity. The convective terms are linearized in the same way for both formulations.

Remark. For Burgers' equation we could even have discarded the convective terms since well-posedness and stability is purely governed by the dissipative terms. (This statement is obvious since there exist a Cole-Hopf transformation for Burgers' equation.) However, we linearize the convective and viscous terms separately. To show the procedure in the hyperbolic–parabolic Navier–Stokes case it is necessary to keep the terms separated in order not to change the number and type of boundary conditions.

To simplify notation we will only study the western boundary of the computational domain (see Fig. 1), and we now replace u' by u. The other boundaries are treated similarly. (We point out that the problem with proving stability for the narrow-stencil approximations are as much a Cauchy problem as it is an initial-boundary value problem, due to the compatibility relation.) Consider the following boundary condition

$$\alpha u + c_{11}u_x + c_{12}u_y = g. \tag{20}$$

To simplify the analysis we assume that the boundary data is homogeneous. (The analysis holds for inhomogeneous data, but introduces unnecessary notation.) We apply the energy method to (19), and with the use of (20) we obtain

$$\frac{\mathrm{d}}{\mathrm{d}t}\|u\|^2 = BT + DI. \tag{21}$$

The contribution from the dissipative terms is given by

$$DI = -\int_0^1 \int_0^1 w^{\mathrm{T}}(C + C^{\mathrm{T}})w\,\mathrm{d}x\,\mathrm{d}y, \quad C = \begin{bmatrix} c_{11} & c_{12} \\ c_{21} & c_{22} \end{bmatrix}, \quad w = \begin{bmatrix} u_x \\ u_y \end{bmatrix}. \tag{22}$$

Parabolicity requires that

$$x^{\mathrm{T}}(C + C^{\mathrm{T}})x \geqslant 0. \tag{23}$$

The boundary term is given by $BT = \int_0^1 (a + 2\alpha)u_w^2 \,\mathrm{d}y$. An energy estimate is obtained (including only the western boundary) if

$$a + 2\alpha \leqslant 0. \tag{24}$$

A semi-discretization of (19) using narrow-diagonal SBP operators D_1, D_2 and the SAT method, can be written as

$$v_t + aD_x v + bD_x v = c_{11}D_{2x}v + c_{12}D_xD_y v + c_{21}D_yD_x v + c_{22}D_{2y}v + \mathrm{SAT}. \tag{25}$$

The discrete version of the boundary condition (20) is given by

$$L^{\mathrm{T}}v = \alpha v_w + c_{11}(S_x v)_w + c_{12}(D_y v)_w = g. \tag{26}$$

The penalty term in (25) is given by $\mathrm{SAT} = \tau H_x^{-1} e_0 \otimes (L^{\mathrm{T}}v - g)$.

Lemma 3.7. *The scheme (25) with homogeneous data is stable, if D_1 and D_2 are compatible, $\tau = 1$, and (23), (24) hold.*

Proof. Let $g = 0$. Multiplying (25) by $v^{\mathrm{T}}\overline{H}$ from the left and adding the transpose lead to

$$\frac{\mathrm{d}}{\mathrm{d}t}\|v\|_{\overline{H}}^2 = -2c_{11}v_w^{\mathrm{T}}H(S_x v)_w(1-\tau) - 2c_{12}v_w^{\mathrm{T}}H(D_y v)_w(1-\tau) + (a + 2\tau\alpha)v_w^{\mathrm{T}}Hv_w + DI - c_{11}v^{\mathrm{T}}R_xH_y v - c_{22}v^{\mathrm{T}}H_xR_y v.$$

The discrete dissipation is given by

$$DI = -\begin{bmatrix} D_x v \\ D_y v \end{bmatrix}^{\mathrm{T}} [\overline{H} \otimes (C + C^{\mathrm{T}})] \begin{bmatrix} D_x v \\ D_y v \end{bmatrix}, \tag{27}$$

which exactly mimics the continuous dissipation (22), except for the highest frequency mode. (This is the dissipation term we obtain employing a wide-stencil approximation of (16).) Here we have used the fact that D_2 and D_1 are compatible, (see Definition 3.1) i.e., that $R \equiv M - D_1^{\mathrm{T}}HD_1$ is positive semi-definite. Hence, the two terms $-c_{11}v^{\mathrm{T}}R_xH_y v - c_{22}v^{\mathrm{T}}H_xR_y v$ introduce a small additional damping (that is not present using a wide-stencil approximation). With $\tau = 1$ we obtain

$$\frac{\mathrm{d}}{\mathrm{d}t}\|v\|_{\overline{H}}^2 = (a + 2\alpha)v_w^{\mathrm{T}}Hv_w + DI - c_{11}v^{\mathrm{T}}R_xH_y v - c_{22}v^{\mathrm{T}}H_xR_y v.$$

This is completely analogous to (21). If (24) holds we obtain a non-growing energy. □

Remark. The semi-discrete approximation of the expanded form does not necessarily mimic the energy estimate of the variable coefficients problem (18), i.e., the linearized problem without freezing the coefficients. This is naturally obtained using a wide-stencil (using the first-derivative SBP operator twice) approximation of the non-split form. Hence, the expanded form introduces lower order terms that can potentially contribute to a non-physical time-growth of the numerical solution. (But the growth will always be bounded, i.e., the approximation is stable.) However, we have strong indications that this is not the case (see (11) in Section 2).

3.3. Stability of the Navier–Stokes equations

We are now ready to tie everything together. The (wide-stencil) semi-discrete approximation of (15) using first-derivative SBP operators D_1 is given by

$$v_t + D_x F + D_y G = D_x(\widetilde{C}_{11}D_x v + \widetilde{C}_{12}D_y v) + D_y(\widetilde{C}_{21}D_x v + \widetilde{C}_{22}D_y v). \tag{28}$$

A narrow-stencil approximation of (15) is given by

$$v_t + D_x F + D_y G = D_{2x}^{(\widetilde{C}_{11})} v + D_x \widetilde{C}_{12} D_y v + D_y \widetilde{C}_{21} D_x v + D_{2y}^{(\widetilde{C}_{22})} v. \tag{29}$$

The linearized and frozen coefficient problem of (15) is given by

$$u_t + A u_x + B u_y = C_{11} u_{xx} + C_{12} u_{xy} + C_{21} u_{xy} + C_{22} u_{yy}, \quad [x, y] \in \Omega, \ t \geqslant 0, \tag{30}$$

where A, B, C_{11}, C_{12}, C_{21} and C_{22} are symmetric constant coefficient 4×4 matrices (see [1]). We assume that (30) is subjected to the well-posed boundary conditions $L^{\mathrm{T}} u = g$ (see for example [4]). We apply the energy method to (30),

$$\frac{\mathrm{d}}{\mathrm{d}t} \|u\|^2 = BT + DI, \tag{31}$$

where

$$DI = -\int_0^1 \int_0^1 w^{\mathrm{T}} (C + C^{\mathrm{T}}) w \, \mathrm{d}x \, \mathrm{d}y, \quad C = \begin{bmatrix} C_{11} & C_{12} \\ C_{21} & C_{22} \end{bmatrix}, \quad w = \begin{bmatrix} u_x \\ u_y \end{bmatrix}, \tag{32}$$

denotes the contribution from the dissipative terms. Parabolicity requires that (23) holds. BT are the bounded boundary terms (see [4] for details).

The (wide-stencil) semi-discrete approximation of (30) is given by

$$v_t + A D_x v + B D_y v = (C_{11} D_x D_x + C_{12} D_x D_y + C_{21} D_y D_x + C_{22} D_y D_y) v + \mathrm{SAT}. \tag{33}$$

The penalty (SAT) term imposes the well-posed boundary conditions $L^{\mathrm{T}} u = g$. Multiplying (33) by $v^{\mathrm{T}} \overline{H} \otimes I_4$ from the left and adding the transpose lead to

$$\frac{\mathrm{d}}{\mathrm{d}t} \|v\|^2_{\overline{H} \otimes I_4} = BT + DI. \tag{34}$$

The discrete dissipation is given by

$$DI = -\begin{bmatrix} D_x \otimes I_4 v \\ D_y \otimes I_4 v \end{bmatrix}^{\mathrm{T}} [\overline{H} \otimes (C + C^{\mathrm{T}})] \begin{bmatrix} D_x \otimes I_4 v \\ D_y \otimes I_4 v \end{bmatrix}, \tag{35}$$

which exactly mimics the physical dissipation (32). Proper tuning of the penalty parameters in SAT yield boundary terms BT that exactly mimic the continuous boundary terms (see [4] for details).

A narrow-stencil approximation of (30) is given by

$$v_t + A D_x v + B D_y v = (C_{11} D_{2x} + C_{12} D_x D_y + C_{21} D_y D_x + C_{22} D_{2y}) v + \mathrm{SAT}. \tag{36}$$

The second main result of this paper is stated in the following theorem:

Theorem 3.8. *Eq. (36) is stable if D_1 and D_2 are compatible and if (33) is stable.*

Proof. The difference between (33) and (36) is the approximation of the two second-derivative terms $C_{11} u_{xx}$ and $C_{22} u_{yy}$. The wide-stencil approximation of the second-derivative operator is given by $D_1 D_1 = H^{-1}(-D_1^{\mathrm{T}} H D_1 + B D_1)$, and the narrow stencil operator is given by $D_2 = H^{-1}(-M + BS)$. BD_1 and BS are equivalent and correspond to the boundary derivative operator that interact with the SAT term in the energy estimate to produce boundary terms BT that exactly mimics the continuous boundary terms (as an example of this interaction see Lemma 3.7). According to Definition 3.1, $M = D_1^{\mathrm{T}} H D_1 + R$, with R positive semi-definite.

Multiplying (36) by $v^{\mathrm{T}} \overline{H} \otimes I_4$ from the left and adding the transpose lead to

$$\frac{\mathrm{d}}{\mathrm{d}t} \|v\|^2_{\overline{H} \otimes I_4} = BT + DI - v^{\mathrm{T}} (\overline{R} + \overline{R}^{\mathrm{T}}) v.$$

The above estimate is identical to (34) except for the additional term $-v^{\mathrm{T}}(\overline{R} + \overline{R}^{\mathrm{T}})v$, where

$$\overline{R} = R_x H_y \otimes C_{11} + H_x R_y \otimes C_{22}.$$

Since D_1 and D_2 are compatible $\overline{R}$ is positive semi-definite. Stability of (36) follows since (33) is stable (see [4]). □

We have shown that the narrow-stencil approximation (36) of the linearized Navier–Stokes equations (30) is stable if D_1 and D_2 are compatible. Strang [20] showed that if the solution of the non-linear differential equation is sufficiently smooth, convergence follows if the linearized approximation is stable, meaning that linear stability is a necessary and sometimes sufficient condition for stability.

4. Computations

The accuracy and stability properties of the narrow- and the wide-stencil approximations are compared by performing numerical simulations of 2-D Burgers' equation and the compressible Navier–Stokes equations in 2-D and 3-D. The convergence rate is calculated as

$$q = \log_{10}\left(\frac{\|w - w^{(h_1)}\|_h}{\|w - w^{(h_2)}\|_h}\right) \Big/ \log_{10}\left(\frac{h_1}{h_2}\right), \tag{37}$$

where w is the analytic solution and $w^{(h_1)}$ the corresponding numerical solution with grid size h_1. $\|w - w^{(h_1)}\|_h$ is the discrete l_2-error. The standard, explicit fourth-order Runge–Kutta method is used for time integration.

4.1. 2-D Burgers' equation

The analytic solution to (17) with $c_{11} = c_{12} = c_{21} = c_{22} = \epsilon$ is

$$u = -a \tanh\left(\frac{a((1-\alpha)x + \alpha y - ct)}{2\epsilon}\right) + c, \tag{38}$$

which describes a 2-D viscous shock. The parameter α defines the propagation angle of the shock, and a, c can be chosen arbitrarily. We solve the problems on a rectangular domain Ω, and choose $\epsilon = 0.1$ such that the solution is well resolved on the grids considered.

A viscous shock solution that moves at a 76° angle across the grid (see Fig. 3) is computed with $a = 1$, $c = 2$ and $\alpha = 0.2$ in (38). Convergence studies for the second-, fourth- and sixth-order accurate narrow- and wide-stencil approximations are shown in Tables 1–3. We integrate to $t = 0.3$.

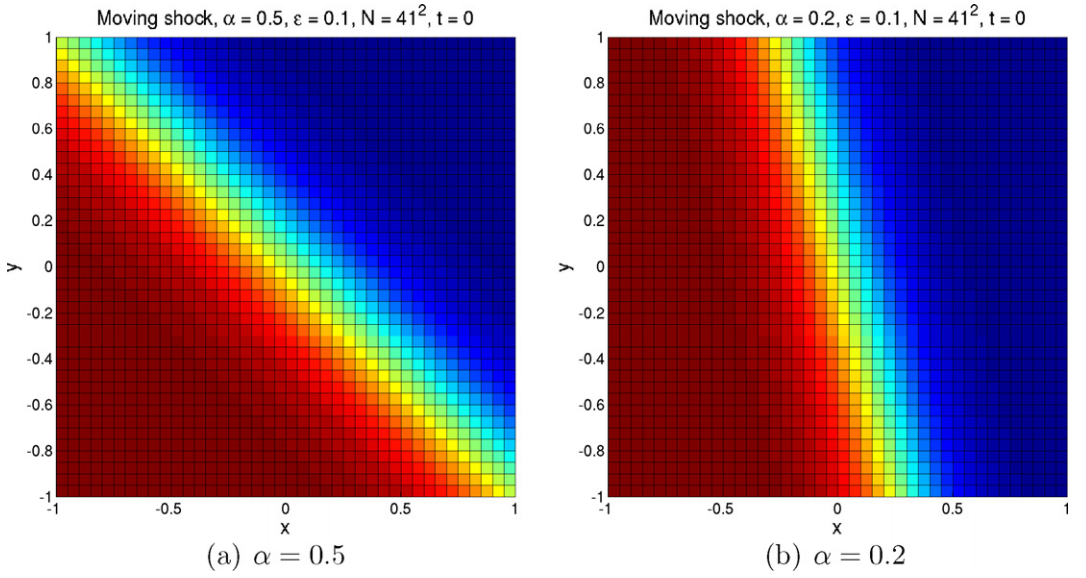

Fig. 3. Initial data for the viscous shock solution to Burgers' equation at two different αs.

Table 1
$\log(l_2 - \text{errors})$ and convergence rates for the second-order narrow- and wide-stencil approximations of Burgers' equation

N, M	$\log l_2^{(\text{narrow})}$	$q^{(\text{narrow})}$	$\log l_2^{(\text{wide})}$	$q^{(\text{wide})}$
21	−2.17		−2.10	
41	−2.81	2.13	−2.74	2.14
61	−3.17	2.08	−3.10	2.05
81	−3.43	2.05	−3.35	2.02

Unsteady solution.

Table 2
$\log(l_2 - \text{error})$ and convergence rates for the fourth-order narrow- and wide-stencil approximations of Burgers' equation

N, M	$\log l_2^{(\text{narrow})}$	$q^{(\text{narrow})}$	$\log l_2^{(\text{wide})}$	$q^{(\text{wide})}$
21	−3.28		−2.85	
41	−4.44	3.86	−3.72	2.89
61	−5.14	3.98	−4.23	2.93
81	−5.64	3.99	−4.60	2.96

Unsteady solution.

Table 3
$\log(l_2 - \text{errors})$ and convergence rates for the sixth-order narrow- and wide-stencil approximations of Burgers' equation

N, M	$\log l_2^{(\text{narrow})}$	$q^{(\text{narrow})}$	$\log l_2^{(\text{wide})}$	$q^{(\text{wide})}$
21	−3.42		−2.99	
41	−4.83	4.70	−4.17	3.94
61	−5.71	4.98	−4.90	4.10
81	−6.34	5.07	−5.42	4.18

Unsteady solution.

There are two sources of numerical errors, dispersive errors from the discretization of the convective terms, and dissipative errors from the discretization of the viscous terms. The major difference between the narrow- and the wide-stencil approximations is the treatment of the non-mixed second-derivative terms. We should not expect to see to much difference in accuracy for problems where the dispersive errors are equal or larger than the dissipative errors. This is true for the second-order case (see Table 1), which has large dispersive errors (due to the error constants of the first-derivative approximations). For higher-order approximations, with much less dispersive errors (see [12]), the narrow-stencil approximations are more accurate than the corresponding wide-stencil approximations, as seen in Tables 1–3. Also the gain in accuracy is higher for steady problems (see Tables 4–6, when the dispersive errors are zero).

A comparison between the fourth-order accurate narrow- and wide-stencil discretizations with $\alpha = 0.2$ (see Fig. 3) where the viscous shock travels out through the north and east boundaries was done. The results are shown in Figs. 4 and 5, indicating the problem for the wide-stencil approximations (without the addition of artificial dissipation to damp the highest frequency mode).

Table 4
$\log(l_2 - \text{errors})$ and convergence rates for the second-order narrow- and wide-stencil approximations of Burgers' equation

N	$\log l_2^{(\text{narrow})}$	$q^{(\text{narrow})}$	$\log l_2^{(\text{wide})}$	$q^{(\text{wide})}$
21	−2.94		−2.43	
41	−3.54	2.01	−3.05	2.06
61	−3.90	2.04	−3.41	2.04
81	−4.16	2.03	−3.66	2.03

Steady solution.

Table 5
$\log(l_2 - \text{errors})$ and convergence rates for the fourth-order narrow- and wide-stencil approximations of Burgers' equation

N	$\log l_2^{(\text{narrow})}$	$q^{(\text{narrow})}$	$\log l_2^{(\text{wide})}$	$q^{(\text{wide})}$
21	−3.58		−2.96	
41	−4.72	3.80	−3.83	2.87
61	−5.44	4.11	−4.37	3.05
81	−5.96	4.10	−4.75	3.06

Steady solution.

Table 6
$\log(l_2 - \text{errors})$ and convergence rates for the sixth-order narrow- and wide-stencil approximations of Burgers' equation

N	$\log l_2^{(\text{narrow})}$	$q^{(\text{narrow})}$	$\log l_2^{(\text{wide})}$	$q^{(\text{wide})}$
21	−3.58		−3.04	
41	−4.97	4.62	−4.21	3.87
61	−5.94	5.54	−4.93	4.14
81	−6.68	5.87	−5.46	4.23

Steady solution.

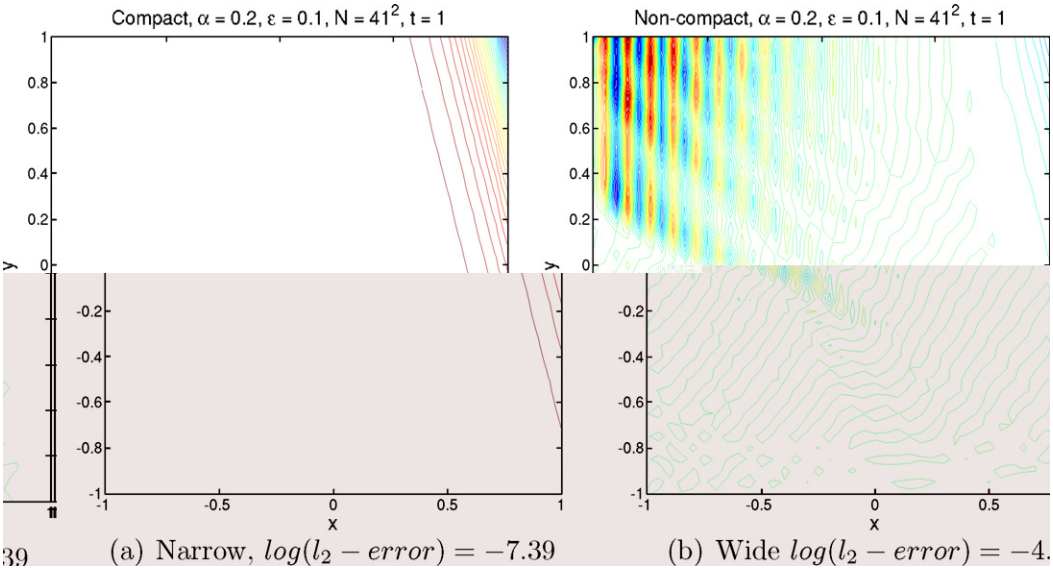

Fig. 4. The shock solution for the fourth-order accurate narrow- and the wide-stencil approximations of Burgers' equation at $t = 1$, after a passage through the north and east boundaries.

Many applications are time-independent (steady-state) problems. A stationary viscous shock is computed with $a = 1$, $c = 0$ in (38). This means that there are no dispersive errors present in the computation, which highlights the dissipative errors. Convergence studies for the second-, fourth- and sixth-order accurate narrow- and wide-stencil discretizations are shown in Tables 4–6. For the second-order accurate case the benefit of using a narrow formulation is now more evident (compare with Table 1).

A leading motive (see Section 1) using a narrow-stencil approximation is to have damping of the highest frequency mode. The spurious oscillations are often triggered by unresolved features in the solution (like a shock). We set $\epsilon = 0.01$ to test the stability and accuracy properties of a mildly under-resolved problem (strong shocks require additional artificial dissipation, also for narrow-stencil approximations). The solutions using the second-order accurate wide- and narrow-stencil approximations are compared. For $N < 100$, this is a slightly under-resolved problem. To obtain a solution with an l_2-error less than 0.01, the second-order

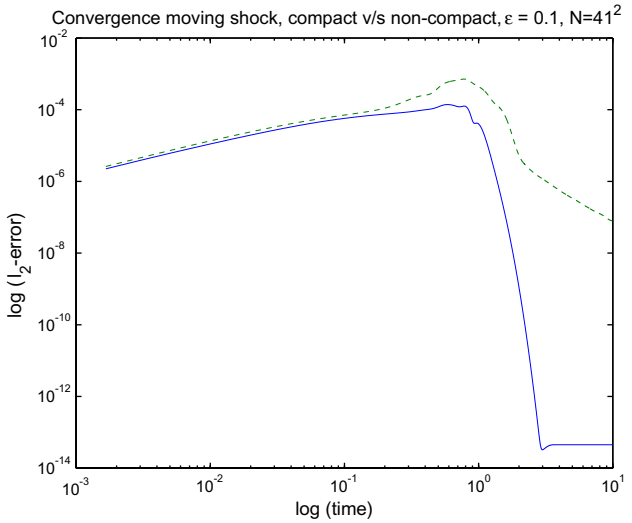

Fig. 5. The convergence histories for a shock passing through the north and east boundaries. The solid and the dashed lines are the fourth-order narrow-stencil and wide-stencil approximations, respectively.

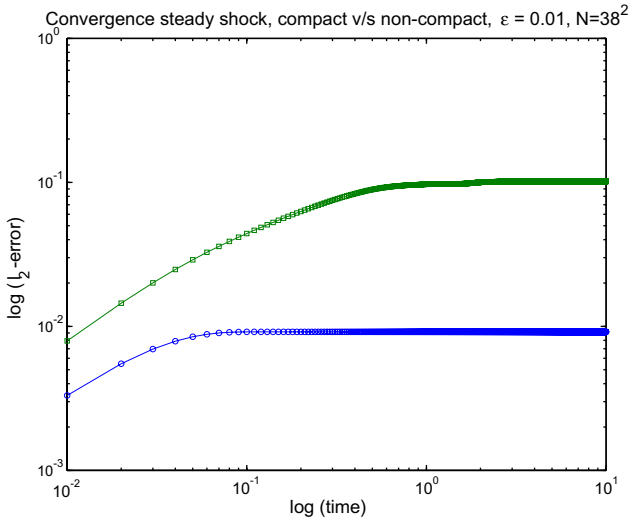

Fig. 6. Convergence history of the second-order accurate narrow- (circles) and wide- (boxes) stencil approximations of Burgers' equation. Steady viscous shock.

narrow-stencil approximation requires 38^2 grid points, and the corresponding wide-stencil approximation requires 94^2 grid points. The difference is due to the presence of the highest frequency mode. In Figs. 6 and 7, we show a comparison between the narrow- and the wide-stencil approximations on the mesh with 38^2 grid points. Both solutions were run to $t = 10$. The highest frequency mode is clearly present in the wide-stencil approximation.

4.2. The compressible Navier–Stokes equations

We begin by computing an analytic viscous shock solution (see [22]) in 2-D. The solution characteristics resemble that of (38), and the computational domain is $0 \leqslant x, y \leqslant 3$. In the first test, we consider a moving viscous shock initiated 0.5 unit lengths away from the diagonal of the box. The shock is propagated with

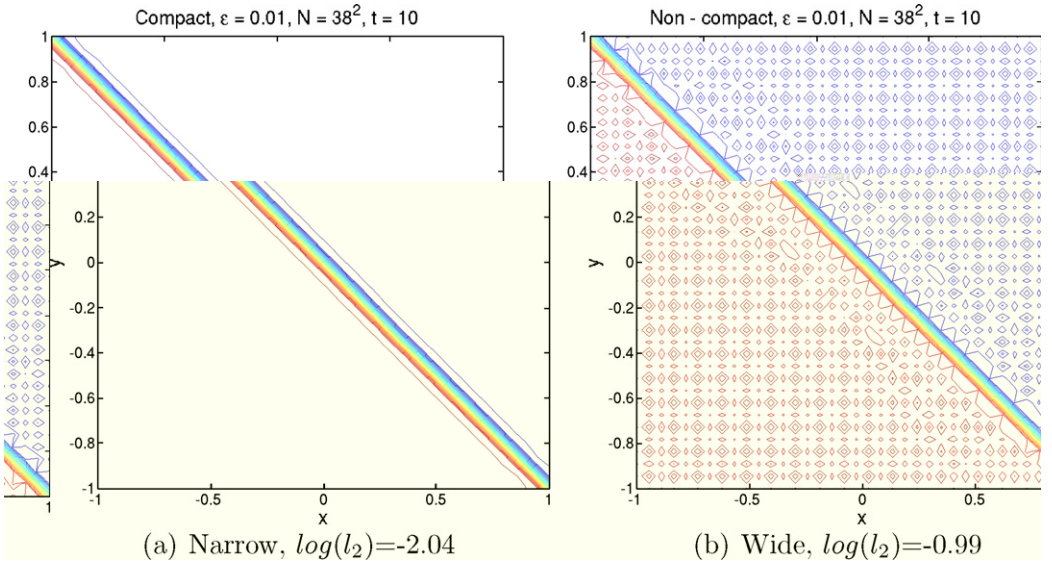

Fig. 7. The second-order accurate narrow- and the wide-stencil solution for the stationary shock at $t = 10$, for Burgers' equation.

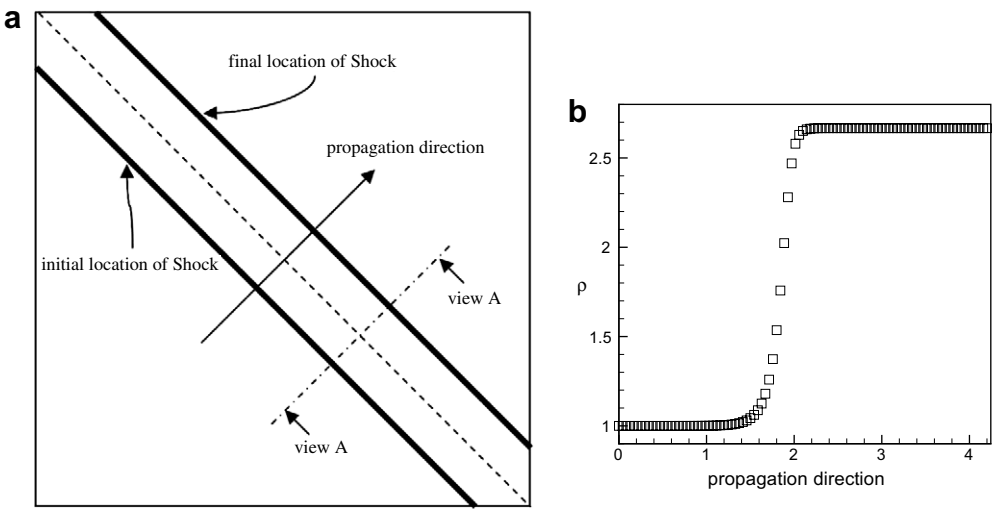

Fig. 8. Schematic of problem setup (a) and initial profile (b). 2-D compressible Navier–Stokes equations.

Table 7
$\log(l_2 - \text{error})$ and convergence rate, q, for the narrow- and wide-stencil approximations of the Navier–Stokes equations, and a moving shock solution

N	$l_2^{(\text{narrow})}$	$q^{(\text{narrow})}$	$l_2^{(\text{wide})}$	$q^{(\text{wide})}$
30	−1.61		−1.43	
60	−2.28	2.22	−2.06	2.07
120	−2.89	2.14	−2.68	2.06
240	−3.50	2.10	−3.28	2.05

an angle of 45°, 1 length units across the grid. The Reynolds number is 10, which results in a smooth profile on this particular grid. The initial profile on the 120×120-grid is shown in Fig. 8. A convergence study is shown in Table 7, where the errors are measured at time $t = 1$.

The difference (in accuracy) between the second-order accurate
are small. This is consistent with the analysis done for Burge
sive errors dominates (the dissipative errors) for the se
would have been larger for higher-order approxi
In the second test the propagation velocity i
avoid the dispersive errors. A convergenc
gers' equation, see Table 4) the gain
As a final test we consider the
pic turbulence is simulated in

$$E(k) = \frac{16}{3}\sqrt{\frac{2}{\pi}} M_{t0}^2 k^4$$

where M_{t0} is the i
over time is fou
tial condition
chosen to h

The si
scale),
The re
pact
unst
usi
di
r

Remark. Both the narrow- and the wide-stencil approximations need artificial dissipation for certain applications to stabilize the solution. This is due to the non-linear terms that may amplify high frequency modes. Since the narrow-stencil approximation has more artificial viscosity built in, it is likely that it will need less extra artificial dissipation than the wide-stencil approximation.

5. Conclusions

We have proven that narrow-stencil approximations of the compressible Navier–Stokes equations are stable, if the first- and second-derivative finite difference operators are compatible. Our approach have been to use SBP operators and the SAT technique to enforce the boundary conditions. It is proven in a number of cases that compatibility can be achieved by proper tuning of the free parameters in the SBP operators.

Numerical computations for both Burgers' equation, and the compressible Navier–Stokes equations in 2-D and 3-D corroborate the stability proofs, and show that a stable narrow-stencil approximation is more accurate and robust than the corresponding wide-stencil approximation.

Appendix A. Proof of Theorem 3.3

Proof. Consider

$$v^{\mathrm{T}}Av = \sum_{i=1}^{n}\sum_{j=1}^{n} v_i A_{ij} v_j = \sum_{i=1}^{n} v_i \left(A_{ii}v_i + \sum_{j\neq i} A_{ij} v_j \right) = \sum_{i=1}^{n} v_i \left(\left(-\sum_{j\neq i} A_{ij} \right) v_i + \sum_{j\neq i} A_{ij} v_j \right)$$
$$= \sum_{i=1}^{n} v_i \left(\sum_{j\neq i} A_{ij}(v_j - v_i) \right).$$

Since $A = A^{\mathrm{T}}$ we have

$$\sum_{i=1}^{n} v_i \left(\sum_{j\neq i} A_{ij}(v_j - v_i) \right) = \sum_{i=1}^{n} \sum_{j>i} (v_i - v_j)^2 (-A_{ij}).$$

Denote the ith row sum by S_i. Then consider

$$S_1 = -\sum_{j>2} A_{1j}(v_2 - v_j)^2 = (-A_{12})(v_1 - v_2)^2 + (-A_{13})(v_1 - v_3)^2$$
$$= (-A_{13})(v_1 - v_2)^2 + (-A_{13})((v_1 - v_2)^2 + (v_2 - v_3)^2 + 2(v_1 - v_2)(v_2 - v_3)).$$

Introduce, $w_i = v_i - v_{i+1}$ such that

$$S_1 = (w_1, w_2) \begin{pmatrix} -A_{12} - A_{13} & -A_{13} \\ -A_{13} & -A_{13} \end{pmatrix} \begin{pmatrix} w_1 \\ w_2 \end{pmatrix}. \tag{40}$$

The structure for all interior row sums follows from (40) and we write

$$S_i = (w_i, w_{i+1}) \begin{pmatrix} -A_{i,i+1} - A_{i,i+2} & -A_{i,i+2} \\ -A_{i,i+2} & -A_{i,i+2} \end{pmatrix} \begin{pmatrix} w_i \\ w_{i+1} \end{pmatrix}. \tag{41}$$

For $i = n - 1$ we have

$$(w_{n-1}, w_n) \begin{pmatrix} -A_{n-1,n} & 0 \\ 0 & 0 \end{pmatrix} \begin{pmatrix} w_{n-1} \\ w_n \end{pmatrix}. \tag{42}$$

(For $i = n$ there is no contribution.) Compute

$$\sum_{i=1}^{n} S_i = v^{\mathrm{T}} A v = w^{\mathrm{T}} B w, \tag{43}$$

where

$$w^{\mathrm{T}} = (w_1, w_2, \ldots, w_n) \tag{44}$$

and

$$B = \begin{pmatrix} -A_{12} - A_{13} & -A_{13} & 0 & \ldots & \\ -A_{13} & -A_{13} - A_{23} - A_{24} & -A_{24} & 0 & \\ 0 & -A_{24} & -A_{24} \ldots & & \\ & & \ddots & & 0 \\ & & & \ldots - A_{n,n-1} - A_{n,n-2} & 0 \\ & & & 0 & 0 \end{pmatrix}.$$

Note that $-A_{12}$ is positive by assumption. If $-A_{12} \geqslant 2A_{13}$, the first row is diagonally dominant. The second row is diagonally dominant if $-A_{23} \geqslant 2A_{13} + 2A_{24}$. The same structure carries through the entire matrix yielding the general condition $-A_{i,i+1} \geqslant 2A_{i-1,i+1} + 2A_{i,i+2}$ for diagonal dominance. Hence, the eigenvalues of B are all positive or 0 and it follows that A is positive semi-definite. □

Appendix B. Proof of Proposition 3.5

Proof. We begin by stating that for all grid sizes we have numerically tested that the R matrices for the fourth-, sixth- and eighth-order schemes are positive semi-definite. Although a strong indication, we cannot formally guarantee by a mere numerical study that this is the case as $h \to 0$. We will give a stronger argument that this is the case using an observation from the second-order proof.

In the second-order case we proved that a matrix A was positive semi-definite via the identity

$$v^{\mathrm{T}} A v = (Dv)^{\mathrm{T}} B (Dv), \tag{45}$$

where D is the non-square matrix

$$D = \begin{pmatrix} -1 & 1 & 0 & \ldots & \\ 0 & -1 & 1 & 0 & \ldots \\ & & \ddots & & \\ & & & -1 & 1 \end{pmatrix}. \tag{46}$$

Semi-definiteness of A then follows from diagonal dominance of B. The action of this operation is that it removes the 0 eigenvalue of A and compresses the penta-diagonal matrix A to a tri-diagonal matrix B. For high-order schemes one could repeat this procedure and compress the matrix further until achieving a diagonally dominant matrix.

Let R denote the remainder matrix $R \equiv M - D_1^{\mathrm{T}} H D_1$. Let D be defined as above and D^{-1} its non-square pseudo-inverse. Multiplication from left and right by a symmetric positive matrix does not change definiteness of R. In this case $D^{-1}D$ is a symmetric positive semi-definite matrix. It has 1 eigenvalue equal to 0. The following algorithm is used to ensure positive semi-definiteness of R.

1. For R being an $n \times n$-matrix, compute the eigenvalues. If k of them is 0 and all the other are positive, continue to (2). (If not the proof fails.)

2. Compute the $(n-1)\times(n-1)$-matrix $R^1 = (D^{-1})^{\mathrm{T}} R D^{-1}$. R^1 has one sub- and super diagonal less than R. Compute the eigenvalues of R^1. They should all be positive except $k-1$ which are 0. (If not the proof fails.) If R^1 is diagonally dominant with the non-negative entries on the diagonal, go to (4), else go to (3).
3. If $k-1>0$ repeat 2) with $R=R^1$ and a reduced size D, else the proof fails.
4. By construction, the rows in the interior of R^1 repeats themselves. Letting $h\to 0$ is equivalent to adding more (identical) rows in the interior of R. Since all rows that are added are diagonally dominant we do not change the definiteness of R^1. Transforming back to R leads to a positive semi-definite R.

Without showing all the details, we conclude that we have tested the above algorithm for the fourth- and sixth-order schemes and reduced the R matrix to a diagonally dominant matrix. For the eighth-order scheme the above algorithm does not lead to a proof since the reduced matrix never becomes diagonally dominant. However, even in the eighth-order case, we stress that R as well as all reduced size R^1s all are positive semi-definite. □

Appendix C. SBP operators

The first-derivative operator is given by $D_1 = H^{-1}Q$ and the second derivative operator $D_2 = H^{-1}(-M+BS)$. Using the first-derivative SBP operator twice, we obtain the following second-derivative SBP operator, $(D_1)^2 = (-D_1^T H D_1 + B D_1)$. D_2 and $(D_1)^2$ have different dissipative terms. The remainder is given by $R = M - D_1^T H D_1$. The operators for the second-, fourth-, sixth- and eighth-order case are given below. For the second-order case we also include the variable diffusion SBP operator.

C.1. Second-order interior and first-order boundary accuracy for D_1 and D_2

The first-derivative operator is defined by

$$H = h\begin{bmatrix} \frac{1}{2} & & & & \\ & 1 & & & \\ & & \ddots & & \\ & & & 1 & 0 \\ & & & & \frac{1}{2} \end{bmatrix}, \quad Q = \begin{bmatrix} -\frac{1}{2} & \frac{1}{2} & & & & & \\ -\frac{1}{2} & 0 & \frac{1}{2} & & & & \\ & & \ddots & & & & \\ & & & -\frac{1}{2} & 0 & \frac{1}{2} & \\ & & & & -\frac{1}{2} & \frac{1}{2} \end{bmatrix}.$$

The narrow second-derivative SBP operator for variable coefficients are given by

$$D_2 = H^{-1}(-D^{\mathrm{T}}\widetilde{B}D + BS),$$

where

$$D = \frac{1}{h}\begin{bmatrix} -1 & 1 & & & \\ & -1 & 1 & & \\ & & \ddots & & \\ & & & -1 & 1 \\ & & & -1 & 1 \end{bmatrix}, \quad \widetilde{B} = \frac{h}{2}\begin{bmatrix} b_0+b_1 & & & & \\ & b_1+b_2 & & & \\ & & \ddots & & \\ & & & b_{N-1}+b_N & \\ & & & & 0 \end{bmatrix}$$

and

$$B = \begin{bmatrix} -b_0 & & & & \\ & 0 & & & \\ & & \ddots & & \\ & & & 0 & \\ & & & & b_N \end{bmatrix}, \quad S = \frac{1}{h}\begin{bmatrix} \frac{3}{2} & -2 & \frac{1}{2} & & & & \\ & 1 & & & & & \\ & & \ddots & & & & \\ & & & & & 1 & \\ & & & & \frac{1}{2} & -2 & \frac{3}{2} \end{bmatrix}.$$

For the special case of constant b we obtain

$$D^{\mathrm{T}}\widetilde{B}D = M = \frac{1}{h}\begin{bmatrix} 1 & -1 & & & & & \\ -1 & 2 & -1 & & & & \\ & & & \ddots & & & \\ & & & & -1 & 2 & -1 \\ & & & & & -1 & 1 \end{bmatrix}$$

and the matrix R is given by (13).

C.2. Fourth-order interior and second-order boundary accuracy for D_1 and D_2

The discrete norm is given by $H = h\,\mathrm{diag}(\frac{17}{48}, \frac{59}{48}, \frac{43}{48}, \frac{49}{48}, 1, \ldots)$. The Q, M and S operators (using 9 points) are given by

$$Q = \begin{bmatrix} -\frac{1}{2} & \frac{59}{96} & -\frac{1}{12} & -\frac{1}{32} & & & & & \\ -\frac{59}{96} & 0 & \frac{59}{96} & & & & & & \\ \frac{1}{12} & -\frac{59}{96} & 0 & \frac{59}{96} & -\frac{1}{12} & & & & \\ \frac{1}{32} & 0 & -\frac{59}{96} & 0 & \frac{2}{3} & -\frac{1}{12} & & & \\ & & \frac{1}{12} & -\frac{2}{3} & 0 & \frac{2}{3} & -\frac{1}{12} & & \\ & & & & \ddots & & & & \\ & & \frac{1}{12} & -\frac{2}{3} & 0 & \frac{2}{3} & -\frac{1}{12} & & \\ & & & \frac{1}{12} & -\frac{2}{3} & 0 & \frac{59}{96} & 0 & -\frac{1}{32} \\ & & & & \frac{1}{12} & -\frac{59}{96} & 0 & \frac{59}{96} & -\frac{1}{12} \\ & & & & & & -\frac{59}{96} & 0 & \frac{59}{96} \\ & & & & & \frac{1}{32} & \frac{1}{12} & -\frac{59}{96} & \frac{1}{2} \end{bmatrix},$$

$$M = \frac{1}{h}\begin{bmatrix} \frac{9}{8} & -\frac{59}{48} & \frac{1}{12} & \frac{1}{48} & & & & & \\ -\frac{59}{48} & \frac{59}{24} & -\frac{59}{48} & & & & & & \\ \frac{1}{12} & -\frac{59}{48} & \frac{55}{24} & -\frac{59}{48} & \frac{1}{12} & & & & \\ \frac{1}{48} & 0 & -\frac{59}{48} & \frac{59}{24} & -\frac{4}{3} & \frac{1}{12} & & & \\ & & \frac{1}{12} & -\frac{4}{3} & \frac{5}{2} & -\frac{4}{3} & \frac{1}{12} & & \\ & & & & \ddots & & & & \\ & & \frac{1}{12} & -\frac{4}{3} & \frac{5}{2} & -\frac{4}{3} & \frac{1}{12} & & \\ & & & \frac{1}{12} & -\frac{4}{3} & \frac{59}{24} & -\frac{59}{48} & 0 & \frac{1}{48} \\ & & & & \frac{1}{12} & -\frac{59}{48} & \frac{55}{24} & -\frac{59}{48} & \frac{1}{12} \\ & & & & & & -\frac{59}{48} & \frac{59}{24} & -\frac{59}{48} \\ & & & & & \frac{1}{48} & \frac{1}{12} & -\frac{59}{48} & \frac{9}{8} \end{bmatrix},$$

$$S = \frac{1}{h}\begin{bmatrix} \frac{11}{6} & -3 & \frac{3}{2} & -\frac{1}{3} & & & & \\ & 1 & & & & & & \\ & & \ddots & & & & & \\ & & & & & 1 & & \\ & & & & -\frac{1}{3} & \frac{3}{2} & -3 & \frac{11}{6} \end{bmatrix}.$$

The left boundary closure for the dissipative term $(M - D_1^{\mathrm{T}} H D_1)/h$ is given by

$$\begin{bmatrix} \frac{59097}{573104} & -\frac{10679}{35088} & \frac{3889}{13328} & -\frac{941}{11696} & -\frac{80}{6321} & \frac{1}{392} & 0 & 0 & 0 & 0 & 0 \\ -\frac{10679}{35088} & \frac{34043}{35088} & -\frac{295}{272} & \frac{16697}{35088} & -\frac{59}{1032} & 0 & 0 & 0 & 0 & 0 & 0 \\ \frac{3889}{13328} & -\frac{295}{272} & \frac{95231}{59976} & -\frac{2891}{2448} & \frac{95}{196} & -\frac{373}{3528} & \frac{1}{144} & 0 & 0 & 0 & 0 \\ -\frac{941}{11696} & \frac{16697}{35088} & -\frac{2891}{2448} & \frac{83293}{52632} & -\frac{3779}{3096} & \frac{19}{36} & -\frac{1}{9} & \frac{1}{144} & 0 & 0 & 0 \\ -\frac{80}{6321} & -\frac{59}{1032} & \frac{95}{196} & -\frac{3779}{3096} & \frac{487117}{303408} & -\frac{1079}{882} & \frac{19}{36} & -\frac{1}{9} & \frac{1}{144} & 0 & 0 \\ \frac{1}{392} & 0 & -\frac{373}{3528} & \frac{19}{36} & -\frac{1079}{882} & \frac{3757}{2352} & -\frac{11}{9} & \frac{19}{36} & -\frac{1}{9} & \frac{1}{144} & 0 \\ 0 & 0 & \frac{1}{144} & -\frac{1}{9} & \frac{19}{36} & -\frac{11}{9} & \frac{115}{72} & -\frac{11}{9} & \frac{19}{36} & -1/9 & \frac{1}{144} \\ & & & \ddots & \ddots & \ddots & \ddots & \ddots & \ddots & \ddots & \ddots \end{bmatrix}.$$

C.3. Sixth-order interior and third-order boundary accuracy for D_1 and D_2

The discrete norm is given by $H = h\,\mathrm{diag}\left(\frac{13649}{43200}, \frac{12013}{8640}, \frac{2711}{4320}, \frac{5359}{4320}, \frac{7877}{8640}, \frac{43801}{43200}, 1, \ldots\right)$. The left boundary closure of Q is given by

$$\begin{aligned} q_{1,1} &= -\tfrac{1}{2} & q_{1,6} &= x_1 - \tfrac{89387}{129600} & q_{3,5} &= -20x_1 + \tfrac{242111}{17280} & q_{5,7} &= -\tfrac{3}{20} \\ q_{1,2} &= x_1 - \tfrac{953}{16200} & q_{2,3} &= 10x_1 - \tfrac{57139}{8640} & q_{3,6} &= 6x_1 - \tfrac{182261}{43200} & q_{5,8} &= \tfrac{1}{60} \\ q_{1,3} &= -4x_1 + \tfrac{715489}{259200} & q_{2,4} &= -20x_1 + \tfrac{745733}{51840} & q_{4,5} &= 10x_1 - \tfrac{165041}{25920} & q_{6,7} &= \tfrac{3}{4} \\ q_{1,4} &= 6x_1 - \tfrac{62639}{14400} & q_{2,5} &= 15x_1 - \tfrac{18343}{1728} & q_{4,6} &= -4x_1 + \tfrac{710473}{259200} & q_{6,8} &= -\tfrac{3}{20} \\ q_{1,5} &= -4x_1 + \tfrac{147127}{51840} & q_{2,6} &= -4x_1 + \tfrac{240569}{86400} & q_{4,7} &= \tfrac{1}{60} & q_{6,9} &= \tfrac{1}{60} \\ & & q_{3,4} &= 20x_1 - \tfrac{176839}{12960} & q_{5,6} &= x_1 & & \end{aligned}$$

In the interior we have the skew-symmetric stencil $(Qv)_j = -\frac{1}{60}v_{j-3} + \frac{3}{20}v_{j-2} - \frac{3}{4}v_{j-1} + \frac{3}{4}v_{j+1} - \frac{3}{20}v_{j+2} + \frac{1}{60}v_{j+3}$. The optimal values of the free parameter is given by

$$x_1 = \frac{342523}{518400}$$

The 5th-order accurate boundary derivative operator is given by

$$S = \frac{1}{h}\begin{bmatrix} \frac{25}{12} & -4 & 3 & -\frac{4}{3} & \frac{1}{4} & & \\ & & 1 & & & & \\ & & & \ddots & & & \\ & & & & 1 & & \\ & & \frac{1}{4} & -\frac{4}{3} & 3 & -4 & \frac{25}{12} \end{bmatrix}.$$

The left boundary closure of $h\,M$ is given by

$$
\begin{array}{llll}
m_{1,1} = \frac{15583}{12960} & m_{2,3} = -\frac{134603}{51840} & m_{3,6} = -\frac{30409}{86400} & m_{5,7} = \frac{3}{20} \\
m_{1,2} = -\frac{253093}{172800} & m_{2,4} = \frac{4141}{2880} & m_{4,4} = \frac{37967}{6480} & m_{5,8} = -\frac{1}{90} \\
m_{1,3} = \frac{52391}{129600} & m_{2,5} = -\frac{86551}{103680} & m_{4,5} = -\frac{53369}{17280} & m_{6,6} = \frac{49}{18} \\
m_{1,4} = -\frac{68603}{259200} & m_{2,6} = \frac{24641}{129600} & m_{4,6} = \frac{54899}{129600} & m_{6,7} = -\frac{3}{2} \\
m_{1,5} = \frac{2351}{14400} & m_{3,3} = \frac{10991}{2160} & m_{4,7} = -\frac{1}{90} & m_{6,8} = \frac{3}{20} \\
m_{1,6} = -\frac{4207}{103680} & m_{3,4} = -\frac{22583}{5184} & m_{5,5} = \frac{2747}{810} & m_{6,9} = -\frac{1}{90} \\
m_{2,2} = \frac{42353}{12960} & m_{3,5} = \frac{46969}{25920} & m_{5,6} = -\frac{820271}{518400} &
\end{array}
$$

In the interior we have the symmetric scheme: $-h(Mv)_j = \frac{1}{90}v_{j-3} - \frac{3}{20}v_{j-2} + \frac{3}{2}v_{j-1} - \frac{49}{18}v_j + \frac{3}{2}v_{j+1} - \frac{3}{20}v_{j+2} + \frac{1}{90}v_{j+3}$.

C.4. Eighth-order interior and fourth-order boundary accuracy for D_1 and D_2

The discrete norm H is defined as

$$
\begin{array}{llll}
H_{1,1} = \frac{1498139}{5080320} & H_{3,3} = \frac{20761}{80640} & H_{5,5} = \frac{299527}{725760} & H_{7,7} = \frac{670091}{725760} \\
H_{2,2} = \frac{1107307}{725760} & H_{4,4} = \frac{1304999}{725760} & H_{6,6} = \frac{103097}{80640} & H_{8,8} = \frac{5127739}{5080320}
\end{array}
$$

The left boundary closure of Q is given by

$$
\begin{array}{ll}
q_{1,1} = -\frac{1}{2} & q_{4,5} = -\frac{47206049}{322560} + 175x_3 + 50x_1 + 175x_2 \\
q_{1,2} = -\frac{15849163}{2257920} + 10x_3 + x_1 + 5x_2 & q_{4,6} = \frac{7628371}{483840} - 40x_1 - 105x_2 \\
q_{1,3} = \frac{235236677}{6773760} - 45x_3 - 5x_1 - 24x_2 & q_{4,7} = \frac{79048289}{1088640} - 105x_3 + 10x_1 \\
q_{1,4} = -\frac{3577778591}{60963840} + 75x_3 + 10x_1 + 45x_2 & q_{4,8} = -\frac{19764155}{677376} + 40x_3 + 10x_2 \\
q_{1,5} = \frac{67906303}{1693440} - 50x_3 - 10x_1 - 40x_2 & q_{5,6} = -\frac{165527}{27648} + 15x_1 + 35x_2 \\
q_{1,6} = -\frac{305821}{193536} + 5x_1 + 15x_2 & q_{5,7} = -\frac{4472029}{193536} + 35x_3 - 5x_1 \\
q_{1,7} = -\frac{13322233}{1244160} + 15x_3 - x_1 & q_{5,8} = \frac{657798011}{60963840} - 15x_3 - 5x_2 \\
q_{1,8} = \frac{24839327}{6773760} - 5x_3 - x_2 & q_{5,9} = -\frac{1}{280} \\
q_{2,3} = -\frac{47167457}{483840} + 126x_3 + 15x_1 + 70x_2 & q_{6,7} = x_1 \\
q_{2,4} = \frac{53224573}{241920} - 280x_3 - 40x_1 - 175x_2 & q_{6,8} = x_2 \\
q_{2,5} = -\frac{211102099}{1244160} + 210x_3 + 45x_1 + 175x_2 & q_{6,9} = \frac{4}{105} \\
q_{2,6} = \frac{3884117}{483840} - 24x_1 - 70x_2 & q_{6,10} = -\frac{1}{280} \\
q_{2,7} = \frac{1202315}{24192} - 70x_3 + 5x_1 & q_{7,8} = x_3 \\
q_{2,8} = -\frac{536324953}{30481920} + 24x_3 + 5x_2 & q_{7,9} = -\frac{1}{5} \\
q_{3,4} = -\frac{120219461}{483840} + 315x_3 + 50x_1 + 210x_2 & q_{7,10} = \frac{4}{105} \\
q_{3,5} = \frac{249289259}{967680} - 315x_3 - 75x_1 - 280x_2 & q_{7,11} = -\frac{1}{280} \\
q_{3,6} = -\frac{290167}{17920} + 45x_1 + 126x_2 & q_{8,9} = \frac{4}{5} \\
q_{3,7} = -\frac{1191611}{13440} + 126x_3 - 10x_1 & q_{8,10} = -\frac{1}{5} \\
q_{3,8} = \frac{7439833}{225792} - 45x_3 - 10x_2 & q_{8,11} = \frac{4}{105} \\
 & q_{8,12} = -\frac{1}{280}
\end{array}
$$

In the interior we have the skew-symmetric stencil $(Qv)_j = \frac{1}{280}v_{j-4} - \frac{4}{105}v_{j-3} + \frac{1}{5}v_{j-2} - \frac{4}{5}v_{j-1} + \frac{4}{5}v_{j+1} - \frac{1}{5}v_{j+2} + \frac{4}{105}v_{j+3} - \frac{1}{280}v_{j+4}$. The optimal values of the free parameters are given by

$$
x_1 = \frac{663}{950} \quad x_2 = \frac{17218045066}{142857142469} \quad x_3 = \frac{2883}{3800}
$$

The fifth-order accurate boundary derivative operator is given by

$$S = \frac{1}{h}\begin{bmatrix} \frac{4723}{2100} & -\frac{839}{175} & \frac{157}{35} & -\frac{278}{105} & \frac{103}{140} & \frac{1}{175} & -\frac{6}{175} & & \\ & & & 1 & & & & & \\ & & & & \ddots & & & & \\ & & & & & 1 & & & \\ & & -\frac{6}{175} & \frac{1}{175} & \frac{103}{140} & -\frac{278}{105} & \frac{157}{35} & -\frac{839}{175} & \frac{4723}{2100} \end{bmatrix}.$$

The left boundary closure of h M is given by

$$\begin{aligned}
& & m_{3,3} &= \tfrac{230744527}{1462987008} & & \\
m_{1,1} &= \tfrac{784878351911}{658344153600} & m_{3,4} &= -\tfrac{423587231}{2438311680} & m_{6,6} &= \tfrac{278531401019}{73149350400} \\
m_{1,2} &= \tfrac{166903006097}{128011363200} & m_{3,5} &= \tfrac{43205598281}{87779220480} & m_{6,7} &= -\tfrac{36895065001}{18287337600} \\
m_{1,3} &= -\tfrac{1567796819}{40963636224} & m_{3,6} &= -\tfrac{2438189281}{3657467520} & m_{6,8} &= \tfrac{137529995233}{614454543360} \\
m_{1,4} &= \tfrac{11872280191}{57605113440} & m_{3,7} &= \tfrac{5124426509}{14629870080} & m_{6,9} &= -\tfrac{8}{315} \\
m_{1,5} &= -\tfrac{181883477}{6400568160} & m_{3,8} &= -\tfrac{2099380193}{30722727168} & m_{6,10} &= \tfrac{1}{560} \\
m_{1,6} &= -\tfrac{5440752167}{128011363200} & m_{4,4} &= \tfrac{4782560143}{1880983296} & m_{7,7} &= \tfrac{118811863211}{41146509600} \\
m_{1,7} &= \tfrac{135555328849}{9216818150400} & m_{4,5} &= -\tfrac{24121280107}{10972402560} & m_{7,8} &= -\tfrac{239073018673}{153613635840} \\
m_{2,2} &= \tfrac{51548757343}{24383116800} & m_{4,6} &= \tfrac{10557998671}{9753246720} & m_{7,9} &= \tfrac{1}{5} \\
m_{2,3} &= -\tfrac{29208451}{548620128} & m_{4,7} &= -\tfrac{43556319241}{65834415360} & m_{7,10} &= -\tfrac{8}{315} \\
m_{2,4} &= -\tfrac{82699112501}{87779220480} & m_{4,8} &= \tfrac{8886055027}{61445454336} & m_{7,11} &= \tfrac{1}{560} \\
m_{2,5} &= \tfrac{85781419}{3657467520} & m_{5,5} &= \tfrac{10455211129}{2925974016} & m_{8,8} &= \tfrac{256250}{90711} \\
m_{2,6} &= \tfrac{14122349173}{54862012800} & m_{5,6} &= -\tfrac{28760793619}{10972402560} & m_{8,9} &= -\tfrac{8}{5} \\
m_{2,7} &= -\tfrac{744007661}{6857751600} & m_{5,7} &= \tfrac{80321706377}{87779220480} & m_{8,10} &= \tfrac{1}{5} \\
m_{2,8} &= \tfrac{173210981}{13654545408} & m_{5,8} &= -\tfrac{4039043579}{25602272640} & m_{8,11} &= -\tfrac{8}{315} \\
& & m_{5,9} &= \tfrac{1}{560} & m_{8,12} &= \tfrac{1}{560}
\end{aligned}$$

In the interior we have the symmetric scheme: $-h(Mv)_j = -\frac{1}{560}v_{j-4} + \frac{8}{315}v_{j-3} - \frac{1}{5}v_{j-2} + \frac{8}{5}v_{j-1} - \frac{205}{72}v_j + \frac{8}{5}v_{j+1} - \frac{1}{5}v_{j+2} + \frac{8}{315}v_{j+3} - \frac{1}{560}v_{j+4}$.

References

[1] Saul Abarbanel, David Gottlieb, Optimal time splitting for two- and three-dimensional Navier–Stokes equations with mixed derivatives, J. Comput. Phys. (1981).

[2] G.A. Blaisdell, N.N. Mansour, W.C. Reynolds, Numerical simulations of compressible homogeneous turbulence, Technical Report TF-50, Thermosci. Div. Mech. Eng., Stanford University, 1991.

[3] M.H. Carpenter, D. Gottlieb, S. Abarbanel, Time-stable boundary conditions for finite-difference schemes solving hyperbolic systems: methodology and application to high-order compact schemes, J. Comput. Phys. 111 (2) (1994).

[4] Magnus Svärd, Mark H. Carpenter, Jan Nordström, A stable high-order finite difference scheme for the compressible Navier–Stokes equations, far-field boundary conditions, J. Comput. Phys. 225 (1) (2007) 1020–1038.

[5] Bertil Gustafsson, Heinz-Otto Kreiss, Joseph Oliger, Time Dependent Problems and Difference Methods, Wiley & Sons, Inc., New York, 1995.

[6] A.E. Honein, P. Moin, Higher entropy conservation and numerical stability of compressible turbulence simulation, J. Comput. Phys. 201 (2004) 531–545.

[7] K.R. Kelly, R.W. Ward, S. Treitel, R.M. Alford, Synthetic seismograms: a finite difference approach, Geophysics 41 (1976) 2–27.

[8] H.-O. Kreiss, G. Scherer, Finite Element and Finite Difference Methods for Hyperbolic Partial Differential Equations, Mathematical Aspects of Finite Elements in Partial Differential Equations, Academic Press, Inc., 1974.

[9] Heinz-Otto Kreiss, Jens Lorenz, Initial Boundary Value Problems and the Navier–Stokes Equations, Academic Press, New York, 1989.

[10] Heinz-Otto Kreiss, Joseph Oliger, Comparison of accurate methods for the integration of hyperbolic equations, Tellus XXIV 3 (1972).

[11] S.K. Lele, Compact finite difference schemes with spectral-like resolution, J. Comput. Phys. 103 (1992) 16–42.

[12] K. Mattsson, M. Svärd, M.H. Carpenter, J. Nordström, High-order accurate computations for unsteady aerodynamics, Comput. Fluids 36 (2006) 636–649.
[13] Ken Mattsson, Jan Nordström, Summation by parts operators for finite difference approximations of second derivatives, J. Comput. Phys. 199 (2) (2004) 503–540.
[14] Ken Mattsson, Jan Nordström, High order finite difference methods for wave propagation in discontinuous media, J. Comput. Phys. 220 (2006) 249–269.
[15] Ken Mattsson, Magnus Svärd, Jan Nordström, Stable and accurate artificial dissipation, J. Sci. Comput. 21 (1) (2004).
[16] J. Nordström, M.H. Carpenter, Boundary and interface conditions for high-order finite-difference methods applied to the Euler and Navier–Stokes equations, J. Comput. Phys. 148 (1999).
[17] Jan Nordström, Accurate solution of the Navier–Stokes equations despite unknown outflow boundary data, J. Comput. Phys. 120 (1995).
[18] Jan Nordström, Magnus Svärd, Well posed boundary conditions for the Navier–Stokes equations, SIAM J. Numer. Anal. 43 (3) (2005) 1231–1255.
[19] Bo Strand, Summation by parts for finite difference approximations for d/dx, J. Comput. Phys. 110 (1994) 47–67.
[20] G. Strang, Accurate partial difference methods II. Non-linear problems, Numer. Math. 6 (1964) 37–46.
[21] Magnus Svärd, Ken Mattsson, Jan Nordström, Steady-state computations using summation-by-parts operators, J. Sci. Comput. 24 (1) (2005) 79–95.
[22] Magnus Svärd, Jan Nordström, On the order of accuracy for difference approximations of initial-boundary value problems, J. Comput. Phys. 218 (10) (2006) 333–352.